THE ASTROPHYSICAL JOURNAL, 576:L131–L135, 2002 September 10

FINDING BLACK HOLES WITH MICROLENSING

ERIC AGOL,[1] MARC KAMIONKOWSKI, LÉON V. E. KOOPMANS, AND ROGER D. BLANDFORD
California Institute of Technology, Mail Code 130-33, 1200 East California Boulevard, Pasadena, CA 91125; agol@tapir.caltech.edu
Received 2002 May 2; accepted 2002 July 29; published 2002 August 8

ABSTRACT

The MACHO and OGLE collaborations have argued that the three longest duration bulge microlensing events are likely caused by nearby black holes, given the small velocities measured with microlensing parallax and nondetection of the lenses. However, these events may be due to lensing by more numerous lower mass stars at greater distances. We find a posteriori probabilities of 76%, 16%, and 4% that the three longest events are black holes, assuming a Salpeter initial mass function (IMF) and a 40 $M_\odot$ cutoff for neutron star progenitors; the numbers depend strongly on the assumed mass function but favor a black hole for the longest event for most standard IMFs. The longest events (>600 days) have an a priori ~26% probability of being black holes for a standard mass function. We propose a new technique for measuring the lens mass function using the mass distribution of long events measured with the Advanced Camera for Surveys on the *Hubble Space Telescope*, the Very Large Telescope Interferometer, the *Space Interferometry Mission*, or the *Global Astrometric Interferometer for Astrophysics*.

Subject headings: black hole physics — Galaxy: stellar content — gravitational lensing

1. INTRODUCTION

Counting the number of black hole stellar remnants in our Galaxy is complicated by their faintness. Only a few dozen of an estimated 10^7–10^9 black holes are observed as X-ray binaries (van den Heuvel 1992). Black hole numbers estimated from stellar population synthesis are inaccurate because of variations in the initial mass function (IMF) with metallicity, uncertainty in the star formation history, and uncertainty in the cutoff mass for neutron star progenitors. To count the bulk of the black holes (isolated or in wide binaries) requires a different observable signature, with the best candidate being gravitational microlensing since it only relies on gravity.

Microlensing events are primarily characterized by the event timescale, $\hat{t} = 2R_{\rm E}/v$, where $R_{\rm E}$ is the Einstein radius in the lens plane, $R_{\rm E} = (4GMc^{-2}D_S xy)^{1/2}$, v is the velocity of the lens perpendicular to the observer-source axis, M is the lensing mass, $D_{L,S}$ are the distances to the lens or the source, $x = D_L/D_S$ is the fraction of the distance of the lens to the source, and $y = 1 - x$. The motion of the Earth causes magnification fluctuations during long events, an effect called "microlensing parallax" (μ-π), allowing one to measure the reduced velocity, $\hat{\boldsymbol{v}} = (\boldsymbol{v}_L - x\boldsymbol{v}_S)/y - \boldsymbol{v}_\odot$ (Gould 1992), where the subscripts L, S, and $\odot$ stand for the lens, source, and solar and the velocities are perpendicular to the lensing axis. Given D_S and $\hat{\boldsymbol{v}}$, the lens mass is then solely a function of x,

$$M(x) = (\hat{v}\hat{t}c)^2 y/(16GxD_S). \quad (1)$$

The mass is 0 for $x = 1$, rising to ∞ for $x = 0$; thus, to estimate M requires knowing x.

Bennett et al. (2002b, hereafter B02b) and Mao et al. (2002, hereafter M02) claim that the three longest duration microlensing events discovered toward the bulge with μ-π measurements are likely black holes. To arrive at this conclusion, they assume that each lens is a member of a population that has a velocity and spatial distribution characteristic of the disk and bulge. Here, in addition, we assume that the lenses are drawn from a population that has a *mass function* characteristic of stellar and stellar remnant populations in the disk and bulge and is independent of x. This latter assumption is not true for young bright disk stars (which do not contain much of the disk mass) but may be true for lower mass stars and compact remnants in the disk and bulge. We then find that the probability that these events are black holes is somewhat reduced.

In § 2, we apply the analysis of B02b to MACHO-99-BLG-22 and estimate the implied total black hole number. In § 3, we include a mass function in our prior for the lens mass. In § 4, we consider the timescale distribution for bulge events and describe how mass measurements of long events may provide an estimate of the lens mass function.

2. MASS ESTIMATE FROM REDUCED VELOCITY ONLY

B02b and M02 present seven microlensing events toward the bulge of the Galaxy with μ-π measurements as shown in Figure 1. These events have greatly decreased χ^2 when the μ-π effect is included and are unlikely to be caused by a binary lens or source.

B02b have computed a distance probability for MACHO-96-BLG-5 and MACHO-98-BLG-6 using a likelihood function that depends on the observed reduced velocity and that assumes that the source is in the bulge. Using equation (1), they find that the most likely masses for the two longest events are greater than 3 $M_\odot$ at 68% confidence. Given that these lenses are not detected as main-sequence stars, they argue that they must be black holes. Using the likelihood function of B02b, we find that the mass probability for MACHO-99-BLG-22 (OGLE-1999-BUL-32) has $M = 11^{+12}_{-6}\ M_\odot$ and a 81% probability of being a black hole using the best-fit parameters of Bennett et al. (2002a, hereafter B02a). This differs from the results of B02a because of different assumed disk and bulge velocity dispersions.

If all three events are due to disk black holes, we can estimate the total number. The detection efficiency, ϵ, for events from 100 to 400 days is 20% (Alcock et al. 2000), which we assume also holds at longer $\hat{t}$ (these events are drawn from the alert sample that has a different selection criterion, so a different ϵ may apply). We have computed the timescale probability for black hole lensing events and find that only ~40% have $\hat{t} >$ 1 yr, so $\epsilon \sim 13\%$. These three events yield $\tau \sim 5 \times 10^{-7} \times (\epsilon/0.1)^{-1}$, implying $N_{\rm total} \sim 5 \times 10^8 (\langle M\rangle/9\ M_\odot)^{-1}(\epsilon/0.1)^{-1}$ disk black holes. This estimate is larger than estimates based

[1] Chandra Fellow.

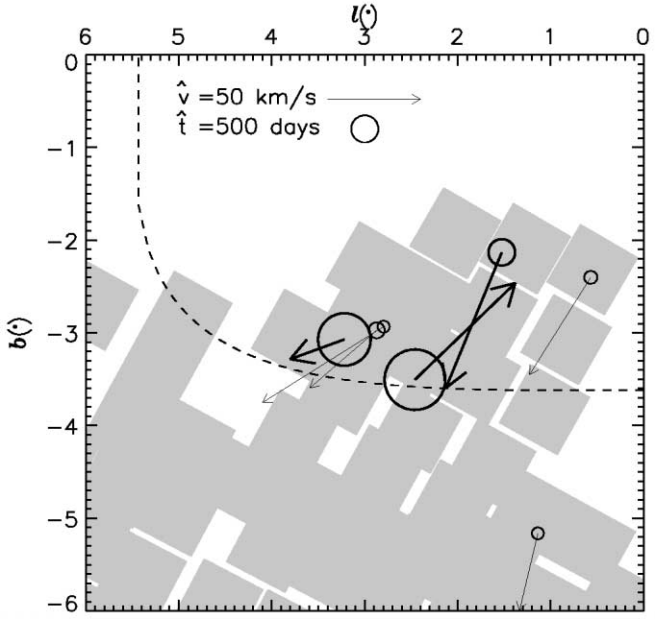

FIG. 1.—Velocity vectors, $\hat{\boldsymbol{v}}$, and event durations, $\hat{t}$ (proportional to circle size), for seven μ-π microlensing events from B02b and M02. The shaded regions show the MACHO bulge fields, while the dashed line shows the region where the bulge density is half of the central bulge density in the sky plane at the distance of the bulge. The boldface symbols indicate three black hole candidate events.

on the expected ratio of the black hole to neutron star remnants, $\sim 10^8$ (Shapiro & Teukolsky 1983; van den Heuvel 1992), and larger than the chemical enrichment by supernovae within the Milky Way, $\sim 2 \times 10^8$ (Samland 1998). This discrepancy indicates that either $\epsilon = 20\%$ is too low, the IMF was much more top heavy in the past, or the events are due to more distant, low-mass stars. We next explore the third option.

3. MASS FUNCTION PRIOR

To recap, the small reduced velocities may indicate that the three longest events most likely lie within 3 kpc and thus should have masses greater than 3 $M_\odot$. However, if a lens is more distant, it is less massive (eq. [1]) and thus drawn from a more abundant population, which can compensate for the small probability of distant lenses having small reduced velocities. Here we investigate the mass likelihood given $\hat{v}$ *and* $\hat{t}$ using the spatial probability $dn_L/dM = \rho(x)\phi(M)/\langle M\rangle$, where $\phi(M)$ is the mass function of a 10 Gyr old stellar population (independent of x), $\int \phi(M)dM = 1$, and $\langle M\rangle = \int dM\, M\phi(M)$ is the mean stellar mass.

To compute $\phi(M)$, we start with the broken power-law IMF from Kroupa (2002) and, following Gould (2000), convert stars with masses $M_{\rm msc} < M < M_{\rm wdc}$ into white dwarfs, $M_{\rm wdc} < M < M_{\rm nsc}$ into neutron stars, and $M_{\rm nsc} < M$ into black holes. We set $M_{\rm msc} = 1\ M_\odot$ and $M_{\rm wdc} = 11\ M_\odot$ (Samland 1998), while we vary $M_{\rm nsc}$. We use Gaussian distributions for the white dwarf and neutron star mass functions with $M_{\rm wd} = 0.5 \pm 0.1\ M_\odot$ (Bragaglia, Renzini, & Bergeron 1995) and $M_{\rm ns} = 1.35 \pm 0.04\ M_\odot$ (Thorsett & Chakrabarty 1999). We describe the black holes with $\phi_{\rm BH} \propto M^{-0.5}$ for $3\ M_\odot < M < 15\ M_\odot$, consistent with the measured mass function of black holes in X-ray binaries (which may have a different mass function than isolated black holes). We compute the relative numbers of each compact remnant by varying the high-mass IMF slope $2 < \beta < 3$, where $\phi_{\rm IMF} \propto M^{-\beta}$, equating the number of each compact remnant with the number of stars in the IMF with appropriate mass range. We assume that this mass function applies in both the disk and the bulge.

The number of black holes depends strongly on the slope of the IMF, β, and on the maximum neutron star progenitor mass, $M_{\rm nsc}$. We choose as a fiducial value, the Salpeter $\beta = 2.35$, consistent with the observed IMF (Kroupa 2002), and $M_{\rm nsc} = 40\ M_\odot$, consistent with chemical-evolution models of the Galaxy (Samland 1998). The resulting mass function has mass fractions of 7% in brown dwarfs, 77% in main-sequence stars, 13% in white dwarfs, 1% in neutron stars, and 1.5% in black holes. This corresponds to a total of about 10^9 neutron stars and 2×10^8 black holes in the Milky Way.

Using Bayes's theorem, the likelihood of a lens being at a given distance x for fixed source distance D_S is $\mathcal{L}(x|\hat{t}, \hat{\boldsymbol{v}}) = \mathcal{L}(\hat{t}, \hat{\boldsymbol{v}}|x)$ for no prior on the distance and no errors on the timescale and velocity measurements. For a survey of duration T covering a solid angle of Ω, then, the solid-angle cross section for magnification greater than 30% by a lens with reduced velocity $\hat{v}$ is $2R_{\rm E}\hat{v}yT/D_L^2$. We must then multiply by the total number of lenses at that distance and integrate over the phase space of the velocity distribution of lenses and sources. We include lenses and sources in the disk and bulge using the bar model described in Dwek et al. (1995) and Han & Gould (1995) and a double-exponential disk with a scale length of 3 kpc, a scale height of 325 pc, a Galactic center distance of 8 kpc, a solar circular velocity of 200 km s^{-1}, a velocity ellipsoid $\sigma_z : \sigma_\phi : \sigma_r = 1 : 1.3 : 2$, $\sigma_z = 17$ km s^{-1} at the solar circle with a scale length of 6 kpc, and an asymmetric drift of $\sigma_r^2/120$ km s^{-1} (Buchalter, Kamionkowski, & Rich 1997). The likelihood function becomes

$$\mathcal{L}(\hat{t}, \hat{\boldsymbol{v}}|x) = N_S \int dM\, d\boldsymbol{v}_S\, d\boldsymbol{v}_L 2R_{\rm E}\hat{v}yT \frac{dn_L}{dM} D_S f(\boldsymbol{v}_L) f(\boldsymbol{v}_S) \times \delta^2[\hat{\boldsymbol{v}}(\boldsymbol{v}_S, \boldsymbol{v}_L, x) - \hat{\boldsymbol{v}}]\delta[\hat{t}(M, \hat{v}, x) - \hat{t}]. \quad (2)$$

The first delta function picks out the particular $\hat{\boldsymbol{v}}$, while the second delta function picks out the particular $\hat{t}$. We convert the velocity delta function in $\hat{\boldsymbol{v}}$ to a delta function in $\boldsymbol{v}_L$, then integrate over $\boldsymbol{v}_L$ and $\boldsymbol{v}_S$, and convert the second delta function to a delta function in mass:

$$\mathcal{L}(\hat{t}, \hat{\boldsymbol{v}}|x) = \frac{N_S 4R_{\rm E}D_S y^3 T\hat{v}}{\hat{t}} \frac{M\phi(M)}{\langle M\rangle} \rho_L \times \left[\exp - \left(\frac{v_l^2}{2\sigma_l^2} + \frac{v_b^2}{2\sigma_b^2}\right) \Big/ 2\pi\sigma_l\sigma_b\right], \quad (3)$$

where $\boldsymbol{v} = (v_l, v_b) = \bar{\boldsymbol{v}}_L - x\bar{\boldsymbol{v}}_S - y(\boldsymbol{v}_\odot + \hat{\boldsymbol{v}})$, $\sigma_{l,b}^2 = \sigma_{L,l,b}^2 + x^2\sigma_{S,l,b}^2$, and l and b denote the components directed in galactic longitude and latitude, respectively. Comparing with the expression in B02b, we see that the likelihood distributions agree if $\phi(M) \propto M^{-3/2}$. We convert from the likelihood of a lens lying at a distance x to a likelihood in M using equation (1). We then integrate over sources at distance D_S using a model for the bulge and disk with luminosity functions measured with the *Hubble Space Telescope* (*HST*). The final constraint is to require that the main-sequence lens stars not exceed the flux limits of B02b and M02 (we ignore the contribution from red giant lenses).

Figure 2 shows the computed mass probability for the above mass function. The white dwarf, neutron star, main-sequence cutoff, and black hole mass cutoff show up as peaks in the

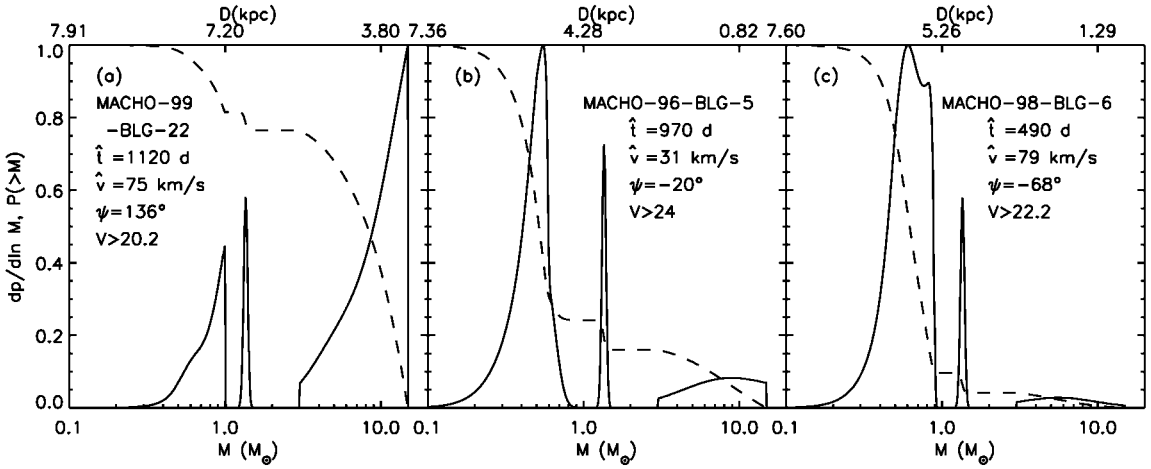

FIG. 2.—Differential (*solid curve*) and integrated (*dashed curve*) likelihood of M given the observed $\hat{\boldsymbol{v}}$ and $\hat{t}$. (*a*) MACHO-99-BLG-22 (OGLE-1999-BUL-32); (*b*) MACHO-96-BLG-5; and (*c*) MACHO-98-BLG-6. The mass function parameters are $\beta = 2.35$ and $M_{\rm nsc} = 40\ M_\odot$. The distance scale at the top of the plots shows $D_L(M)$ *if* $D_S = 8$ kpc. The angle ψ is the velocity direction in Galactic coordinates measured from the rotation direction toward the north Galactic pole. The *V*-band flux limits are from (*a*) M02, (*b*) B02a, and (*c*) B02b.

probability distribution. The greater number of lenses at small mass compensates for the decreased probability for low-$\hat{v}$ events, biasing the probability toward smaller mass. The probability that each lens is a black hole, defined as $M > 3\ M_\odot$, is changed from above: 4% for MACHO-98-BLG-6, 16% for MACHO-96-BLG-5, and 76% for MACHO-99-BUL-22. MACHO-98-BLG-6 and MACHO-96-BLG-5 are most likely main-sequence stars or white dwarf stars at greater than 4 kpc; better flux limits may rule out a main-sequence star. These probabilities change by 1 order of magnitude depending on β and $M_{\rm nsc}$, as shown in Table 1 (the labels are MACHO-XX-BLG-XX, while the first event is also OGLE-1999-BUL-32). The first two columns describe the assumed mass function, the third, fourth, and fifth columns give the black hole probability for each event labeled by their MACHO event number, while the last two columns give the average of $M^{1/2}$ and M^2 for black holes divided by the average for all stars given the assumed IMF.

4. PROBABILITY OF LONG-TIMESCALE LENSING

We next compute the expected distribution of events as a function of timescale. For long timescales, the a priori differential probability distribution scales as $\hat{t}^{-4}$ (Mao & Paczyński 1996). For solar mass stars in the disk and bulge, this behavior occurs for $\hat{t} > 200$ days. We can rescale the probability distribution for different masses

$$\frac{d^2p}{dM\,d\hat{t}} = \langle M\rangle^{-1}\phi(M)\,\frac{dp(M_\odot)}{d(\hat{t}M^{-1/2})}, \qquad (4)$$

TABLE 1
BLACK HOLE PROBABILITIES

β	$M_{\rm nsc}$ ($M_\odot$)	P (%) 99-22	96-5	98-6	$\langle M_{\rm BH}^{1/2}\rangle/\langle M^{1/2}\rangle$	$\langle M_{\rm BH}^{2}\rangle/\langle M^{2}\rangle$
2	20	97	65	30	3E−2	0.78
	40	92	45	17	1.5E−2	0.64
2.35	20	90	33	10	7E−3	0.48
	40	76	16	4	3E−3	0.26
3	20	46	4	1	5E−4	0.07
	40	18	1	0.2	1E−4	0.02

where M is measured in units of $M_\odot$ and $dp(M_\odot)/d\hat{t}$ is the timescale probability distribution, assuming all lenses have mass $M_\odot$. Since at long timescales $dp(M_\odot)/d\hat{t}$ scales as $\hat{t}^{-4}$, we can rescale this equation and integrate over mass

$$\frac{dp}{d\hat{t}} = \int_{M_1}^{M_2}\frac{d^2p}{dM\,d\hat{t}}\,dM \propto \hat{t}^{-4}\int_{M_1}^{M_2} dM\,\phi(M)M^2, \qquad (5)$$

for $\hat{t} > 200M_2^{1/2}$ days. The fraction of all microlensing events as a function of mass scales as $M^{1/2}\phi(M)$, while the fraction of events in the long-timescale tail scales as $M^2\phi(M)$, strongly favoring black holes. Table 1 shows the average of $M^{1/2}$ and M^2 for black holes divided by the mass function average, showing that the fraction of black hole events in the long-timescale tail is increased by 1–2 orders of magnitude as compared with the total number of events. *Thus, with a measurement of the mass distribution of events at long timescales, one can directly infer the mass function if it is independent of the location in phase space.*

We have computed the probability distribution for lensing by solar mass stars (see Han & Gould 1995, 1996 for the computation technique) and then convolved it with our assumed mass function to give the timescale distribution. This is compared with the observed distribution of MACHO events in Figure 3. We have binned the 252 alert events from MACHO[2] and then computed $\hat{t}^2 dn/d\hat{t}$ as $N_i\hat{t}_i^2/(\epsilon_i\Delta\hat{t}_i)$, where i denotes the number of the bin; the errors are Poisson errors. Since the efficiencies, ϵ_i, have not been measured for the alert events, we have used the efficiency curve from Alcock et al. (2000), extrapolating to a longer timescale. We note that the alert event timescales may be affected by blending and that a full analysis of efficiencies is required. The rise at long timescales may indicate that at 20%, the efficiency is underestimated or that the longest two events are a statistical fluke. An efficiency of 100% is indicated for the last three bins by arrows in Figure 3. Decreasing β to 2 improves the agreement for the shorter timescales, but the longest event still lies well above the predicted value, so it may be an improbable event.

We have tried to explain the rise at long timescale by varying

[2] See http://darkstar.astro.washington.edu.

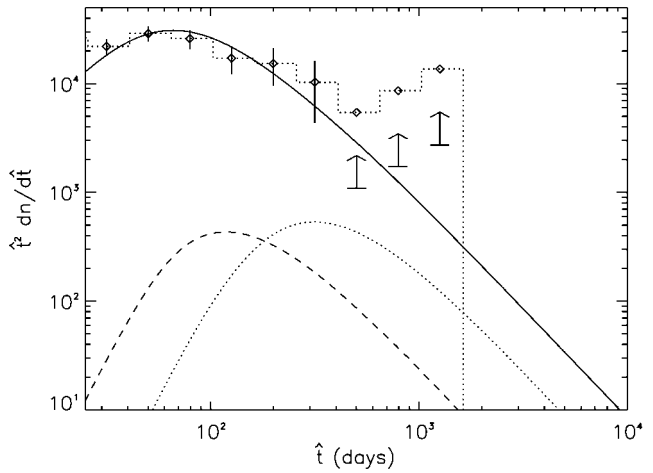

FIG. 3.—Distribution of event timescales, $\hat{t}^2\, dn/d\hat{t}$. The histogram shows the MACHO alert events, while the lines show the predicted distribution for all masses (*solid line*), neutron stars (*dashed line*), and black holes (*dotted line*) for the fiducial IMF.

the assumptions in the Galactic kinematics and density, but all reasonable modifications fail. To explain this discrepancy with a different mass function requires stars of mass $\sim 100\ M_\odot$ since the timescale scales as $M^{1/2}$ and since the probability distribution peaks at ~100 days for $1\ M_\odot$ lenses. However, $100\ M_\odot$ lenses are ruled out by the μ-π observations that indicate that the three longest timescale events would have to be within a few hundred parsecs. This would require an even larger black hole mass density to explain the number of these events, $\sim 1\ M_\odot\ \mathrm{pc}^{-3}$, which exceeds the Oort limit. Also, for events near the peak of the timescale distribution for $100\ M_\odot$ lenses, $\hat{v}$ should be much larger than observed.

5. CONCLUSIONS

We have shown that including the timescale as a constraint on the black hole probability may change the conclusion as to whether or not the lens is a black hole. The probability is most robust for MACHO-99-BLG-22, which is most likely a black hole for the range of mass functions we have explored, while the probability for MACHO-98-BLG-6 and MACHO-96-BLG-5 is strongly dependent on the assumed mass function. A μ-π measurement does not provide sufficient information to estimate the mass of a given event but may result in interesting limits on the mass.

The contribution of a given population of stars to the long-timescale tail ($\hat{t} > 200 M^{1/2}$ days) of the lensing distribution depends on $\langle M^2 \rangle$ for that population. Due to their larger mass, ~26% of events with $\hat{t} > 600$ days should be black hole lenses for $\beta = 2.35$ and $M_{\rm nsc} = 40\ M_\odot$; this fraction may be reduced if black holes have a velocity dispersion much larger than that of disk and bulge stars. Constraining β and $M_{\rm nsc}$ with the timescale distribution will require more events and a careful estimate of the microlens detection efficiency as a function of $\hat{t}$. The parallax events may have an increased efficiency since they are less affected by observing gaps and have a wider cross section as a result of the Earth's motion (B02b).

The OGLE III project may detect 10^3 microlensing events toward the bulge each year (B. Paczyński 2002, private communication), which should include approximately three black hole lensing events and approximately five neutron star events for $\beta = 2.35$ and $M_{\rm nsc} = 40\ M_\odot$. Since the timescale of black hole events is longer, μ-π measurements are feasible from the ground (as demonstrated by B02b). If these can be followed up with astrometric observations, then the mass can be determined when combined with μ-π information (Paczyński 1998; Gould 2001; Boden, Shao, & van Buren 1998). Since the typical mass of black holes, $\sim 9\ M_\odot$, is much higher than the typical lens mass, $\sim 0.5\ M_\odot$, the typical astrometric signal for black hole lens events with a source in the bulge will be ~3 mas, which will easily be measured with the Advanced Camera for Surveys on *HST* (M02), the Very Large Telescope Interferometer (by 2004; Delplancke, Górski, & Richichi 2001), the *Space Interferometry Mission* (by 2009), or the *Global Astrometric Interferometer for Astrophysics* (by 2010–2012; Belokurov & Evans 2002), compared with 0.7 mas for a typical main-sequence lens. The deviation of the centroid is $\delta\theta = \theta_{\rm E}\boldsymbol{u}/(u^2+2)$, where $\boldsymbol{u}$ is the normalized impact parameter as a function of time and $\theta_{\rm E}$ is the Einstein angle (Paczyński 1998). Since $\boldsymbol{u}$ is determined by the photometric light curve, observations of $\delta\theta$ at two different $\boldsymbol{u}$ will suffice to determine $\theta_{\rm E}$. The projected Einstein radius, $\hat{R}_{\rm E} = \hat{v}\hat{t}/2$, can be measured from photometric μ-π variations, allowing one to determine the mass of the lens, $M = c^2 \hat{R}_{\rm E}\theta_{\rm E}/(4G)$. With mass measurements for many long-timescale events, the mass function can be deduced since the probability for lensing is proportional to $\hat{t}^{-4} M^2 \phi(M)$ for a phase-space distribution that is independent of mass (eq. [3]). The M^2 dependence means that detection of black holes will be favored so that one can constrain β and $M_{\rm nsc}$.

Finally, direct observations of the lenses provide another avenue toward determining their nature. If they are black holes, they may accrete from the interstellar medium or from a companion wind. With plausible assumptions, the X-ray radiation could be detectable with current space-based observatories (Agol & Kamionkowski 2002).

We thank Dave Bennett and Shude Mao for constructive comments. This work was supported in part by NSF AAST-0096023, NASA NAG5-8506, and DoE DE-FG03-92-ER40701. E. A. was supported by NASA through Chandra Postdoctoral Fellowship Award PF0-10013 issued by the *Chandra X-Ray Observatory* Center, which is operated by the Smithsonian Astrophysical Observatory for and on behalf of NASA under contract NAS8-39073.

REFERENCES

Agol, E., & Kamionkowski, M. 2002, MNRAS, 334, 553
Alcock, C., et al. 2000, ApJ, 541, 734
Belokurov, V. A., & Evans, N. W. 2002, MNRAS, 331, 649
Bennett, D. P., Becker, A. C., Calitz, J. J., Johnson, B. R., Laws, C., Quinn, J. L., Rhie, S. H., & Sutherland, W. 2002a, preprint (astro-ph/0207006) (B02a)
Bennett, D. P., et al. 2002b, ApJ, in press (astro-ph/0109467) (B02b)
Boden, A. F., Shao, M., & van Buren, D. 1998, ApJ, 502, 538
Bragaglia, A., Renzini, A., & Bergeron, P. 1995, ApJ, 443, 735
Buchalter, A., Kamionkowski, M., & Rich, M. 1997, ApJ, 482, 782
Delplancke, F., Górski, K. M., & Richichi, A. 2001, A&A, 375, 701
Dwek, E., et al. 1995, ApJ, 445, 716
Gould, A. 1992, ApJ, 392, 442
———. 2000, ApJ, 535, 928
———. 2001, PASP, 113, 903
Han, C., & Gould, A. 1995, ApJ, 447, 53
———. 1996, ApJ, 467, 540
Kroupa, P. 2002, Science, 295, 82
Mao, S., & Paczyński, B. 1996, ApJ, 473, 57

Mao, S., et al. 2002, MNRAS, 329, 349 (M02)
Paczyński, B. 1998, ApJ, 494, L23
Samland, M. 1998, ApJ, 496, 155
Shapiro, S. L., & Teukolsky, S. A. 1983, Black Holes, White Dwarfs, and Neutron Stars (New York: Wiley-Interscience)
Thorsett, S. E., & Chakrabarty, D. 1999, ApJ, 512, 288
van den Heuvel, E. P. J. 1992, in Environment Observation and Climate Modelling through International Space Projects, Vol. 3, ed. T. Guyenne & J. Hunt (Noordwijk: ESA/ESTEC), 77